Voltage clamp analysis of acetylcholine produced end-plate current fluctuations at frog neuromuscular junction

C. R. Anderson and C. F. Stevens

J. Physiol. 1973;235;655-691

J. Physiol. (1973), **235**, *pp.* 655–691
With 13 *text-figures*
Printed in Great Britain

VOLTAGE CLAMP ANALYSIS OF ACETYLCHOLINE PRODUCED END-PLATE CURRENT FLUCTUATIONS AT FROG NEUROMUSCULAR JUNCTION

BY C. R. ANDERSON* AND C. F. STEVENS

From the Department of Physiology and Biophysics, University of Washington School of Medicine, Seattle, Washington 98195, U.S.A.

(*Received 30 April 1973*)

SUMMARY

1. Acetylcholine produced end-plate current (e.p.c.) noise is shown to be the results of statistical fluctuations in the ionic conductance of voltage clamped end-plates of *Rana pipiens*.

2. These e.p.c. fluctuations are characterized by their e.p.c. spectra which conform to a relation predicted from a simple model of end-plate channel gating behaviour.

3. The rate constant of channel closing α is determined from e.p.c. spectra and is found to depend on membrane potential V according to the relation $\alpha = Be^{AV}$ ($B = 0{\cdot}17$ msec$^{-1} \pm 0{\cdot}04$ S.E., $A = 0{\cdot}0058$ mV$^{-1} \pm 0{\cdot}0009$ S.E. at 8° C) and to vary with temperature T with a $Q_{10} = 2{\cdot}77$, at -70 mV. A and B in this expression both vary with T and therefore produce a membrane potential dependent Q_{10} for α.

4. Nerve-evoked e.p.c.s and spontaneous miniature e.p.c.s decay exponentially in time with a rate constant which depends exponentially on V. The magnitude and voltage dependence of this decay constant is exactly that found from e.p.c. spectra for the channel closing rate α.

5. The conductance γ of a single open end-plate channel has been estimated from e.p.c. spectra and is found not to be detectibly dependent on membrane potential, temperature and mean end-plate current. $\gamma = 0{\cdot}32 \pm 0{\cdot}0045$ (S.E.) $\times 10^{-10}$ mhos. Some variation in values for γ occurs from muscle to muscle.

6. It is concluded that the relaxation kinetics of open ACh sensitive ionic channels is the rate limiting step in the decay of synaptic current and that this channel closing has a single time constant. The relaxation rate is independent of how it is estimated (ACh produced e.p.c. fluctuations,

* Present address: Physiology Laboratory der Rijksuniversiteit te Leiden, Wassenaarseweg 62, Leiden, The Netherlands.

e.p.c., m.e.p.c.), and is consistent with the hypothesis that individual ionic channels open rapidly to a specific conductance which remains constant for an exponentially distributed duration.

7. The voltage and temperature dependence of the channel closing rate constant agree with the predictions of a simple dipole-conformation change model.

INTRODUCTION

The kinetics of frog end-plate response to acetylcholine (ACh) have standardly been investigated using evoked and spontaneous release of transmitter. These studies are complicated, however, by the fact that the time course of ACh concentration at the post-junctional membrane is unknown. This uncertainty about cleft ACh concentrations inevitably makes any mechanistic interpretation of end-plate current difficult.

For many physical systems, inferences about the responses to stimulation may be made from observations on spontaneous fluctuations; such inferences are possible whenever the relaxation toward equilibrium follows the same course for spontaneously occurring and externally produced perturbations (see Kubo, 1957). The discovery by Katz & Miledi (1970, 1971, 1972, 1973) of 'ACh noise' arising from end-plate conductance fluctuations thus raises the possibility of investigating end-plate channel kinetic behaviour through the properties of end-plate current (e.p.c.) fluctuations observed at constant ACh concentrations, thereby circumventing some of the difficulties inherent in the use of axonal release of ACh.

In an effort to study post-junctional gating kinetics without the complications that arise with nerve-evoked transmitter release, we have carried out a voltage clamp analysis of the end-plate conductance fluctuations produced by constant ACh concentrations. Since post-junctional membrane potential has been demonstrated to alter the time course of end-plate currents (Gage & Armstrong, 1968; Kordas, 1969, 1972*a*, *b*; Magleby & Stevens, 1972*a*), and has been hypothesized to exert its effect through the gating mechanism itself (Magleby & Stevens, 1972*b*), we have been particularly concerned with using this variable as a tool to investigate gating behaviour.

Our results are given in two parts. In the first part we demonstrate that ACh produced e.p.c. fluctuations may indeed be studied with the voltage clamp technique (Takeuchi & Takeuchi, 1959), and present some properties of these e.p.c. fluctuations.

We have described e.p.c. fluctuations in terms of their spectra, a characterization which basically indicates the amplitude of each frequency component present in the fluctuating current. More specifically, an e.p.c. spectrum is calculated by decomposing a record of e.p.c. as a function of

time into constituent sine and cosine components with Fourier analysis; the sum of the squared amplitudes of the resulting sine and cosine waves give the spectral magnitude at the sinusoid frequencies. If the e.p.c. fluctuations are very rapid, for example, relatively large values of spectral estimates will occur even into high frequencies, whereas a slowly varying e.p.c. will have appreciable values for spectral estimates only in the lower frequency range. Altogether, then, the e.p.c. spectrum gives a profile of membrane permeability changes in terms of constituent frequency components, and is rather like the characterization of an amplifier's performance by its frequency response.

Inferences about end-plate conductance mechanisms can be made from e.p.c. fluctuations only through some hypothesis about the source of the e.p.c. fluctuations. In the second part of the Results we have presented a theory of post-junctional events together with a number of predictions about e.p.c. spectra based upon this theory, and have compared these predictions with experimental observations.

The satisfactory agreement we have found between predictions and observations supports the following conclusions: e.p.c. fluctuations reflect the probabilistic opening and closing of end-plate channels each with an open conductance of approximately 2 to 3×10^{-11} mhos. The closing rate of these channels depends exponentially on membrane potential and is the same when measured by e.p.c. spectra or from the closing of channels after axonal release of transmitter quanta. Altogether, ACh produced e.p.c. fluctuations seem to provide a satisfactory means for studying the kinetics of post-junctional conductance mechanisms under conditions of constant ACh concentration.

Some of these results have appeared previously in abstract form (Anderson & Stevens, 1972, 1973).

METHODS

The *Rana pipiens* sartorius nerve-muscle preparation was dissected and maintained in buffered Ringer solution adjusted to pH 7·20 (composition: 117 mM-Na^+, 1·8 mM-Ca^{2+}, 2·5 mM-K^+, 121·1 mM-Cl^-, 0·425 mM-$H_2PO_4^-$, 1·58 mM-HPO_4^{2-}). Experiments were performed on frogs that had been kept at room temperature under running cold tap water for 1 day to 3 weeks. Muscles were pre-treated with either glycerol (Howell & Jenden, 1967) or ethylene glycol (Sevcik & Narahashi, 1972) in order to disrupt excitation–contraction coupling.

The following procedures were used for hypertonic treatment. Steps (1) and (2) at room temperature (22° C):

(1) 50 min, 50 ml., 750–800 mM glycerol in buffered Ringer, pH 7·2; or, 50 min, 50 ml., 1000 mM ethylene glycol in buffered Ringer, pH 7·2.

(2) Then 60 min, 250 ml., Gage & Eisenberg Ringer: 117 M-Na^+, 2·5 mM-K^+, 5 mM-Ca^{2+}, 5 mM-Mg^{2+}, all as chlorides, unbuffered pH 6·8

(3) Finally, experiment, 6 ml., buffered Ringer/pH 7·2, cooled (< 4 hr).

Although glycerol was used in the initial experiments, we came to prefer the

ethylene glycol method because it seemed to yield high resting potentials ($V = -70$ mV *vs.* -40 mV) and larger input resistances. The high concentrations of ethylene glycol and glycerol and particularly the higher temperatures (as compared to those reported in the literature) were critical in producing a muscle whose deep fibres did not contract during nerve stimulation over the 2–4 hr duration of the experiments. The high Ca^{2+}, Mg^{2+} Ringer (Eisenberg *et al.* 1971) seemed to improve both input resistance and resting potential; low pH (6·2–6·8) occasionally produced similar results.

After this treatment the muscle was stretched to its *in situ* length and mounted on the bottom of a glass and wax frame which fitted into a chamber with a standard glass microscope slide base. The resulting close approximation of the muscle to the bottom of the dish provided firm mechanical support and permitted Kohler trans-illumination. The nerve was stimulated through a suction electrode; stimulating current was supplied through an electro-optical isolation unit as pulses of 0·05 msec duration and amplitude adjusted to be supramaximal. Bath temperature was continuously measured with a thermistor positioned near the end-plate region and maintained at the selected value ($\pm$ 0·25° C) by two peltier coolers (CAMBION, Inc.) supplied from a storage battery.

The preparation was usually maintained at temperatures near 10° C for several reasons. First, the low spontaneous quantal release rate (Fatt & Katz, 1952) at these temperatures minimized contributions of miniature end-plate currents to the ACh induced current fluctuations. Secondly, the cut-off frequency of the ACh current fluctuation spectrum was shifted at low temperatures to the frequencies at which extraneous noise arising in the measuring apparatus (see p. 662) was at a minimum ($<$ 200 Hz).

Surface fibres were impaled with two glass micro-electrodes filled with 2·5 M-KCl one for passing current, the other for measuring membrane potential; electrode separation was less than 50 μm. Low impedance voltage recording electrodes (1–5 MΩ) were used to reduce the thermal noise contribution in the voltage clamp records and to improve clamp frequency response. The level of Ringer solution in the chamber was lowered to near the muscle surface ($\sim$ 2 mm) to minimize electrode-bath capacitive coupling, but other precautions in this regards (such as placing a shield between electrodes) proved to be unnecessary for adequate response over the frequency range of interest (0 $\rightarrow$ 500 Hz). A third micro-electrode, for iontophoresis, filled with approximately 2·5 M-ACh chloride was positioned extracellularly near the end-plate region.

Because accurate estimation of end-plate conductance with the voltage clamp techniques require that voltage control over the end-plate be as uniform as possible, care was taken to obtain optimal electrode placement (Takeuchi & Takeuchi, 1959; Gage & McBurney, 1972). A successful penetration showed spontaneous miniature end-plate potentials (m.e.p.p.s) of at least 0·5 mV amplitude and fast rise time which were clearly identifiable simultaneously in both intracellular electrodes. Because membrane potential is not a faithful representation of the underlying conductance changes, final positioning criteria were based upon characteristics of miniature end-plate currents (m.e.p.c.) and evoked end-plate currents (m.e.p.c.) and evoked end-plate currents (e.p.c.) measured under voltage clamp. M.e.p.c. rise times less than about 0·5 msec (T = 10° C.) and peak amplitudes greater than 1 nA at $V = -70$ mV were deemed acceptable. Likewise e.p.c. rise times of approximately 1·5 msec and peak current $>$ 100 nA at -70 mV and 10° C were taken to indicate adequate positioning. End-plates with high m.e.p.c. rates ($>$ 1/sec at 18° C) were rejected to minimize contamination of the ACh spectra.

Because the frog end-plate varies considerably in length (McMahan *et al.* 1972; Peper & McMahan, 1972; see Kuno *et al.* 1971) the uniformity of voltage control

probably varied somewhat from end-plate to end-plate; for example, with end-plate lengths for 15–400 μm and a muscle length constant of 2·5 mm (Fatt & Katz, 1951) terminals would occupy from 0·01 to 0·18 space constants, and the maximum voltage errors would range from 1 to 16% (d.c.). Without visual identification of end-plate dimensions, electrical criteria were used exclusively to judge the adequacy of a clamp. These criteria included the m.e.p.c. and e.p.c. rise times mentioned above and the requirement that residual voltage change during an e.p.c. always be less than 5% of the driving potential.

The iontophoresis electrode was positioned near the point of entry of the intracellular electrodes and test pulses of ACh passed. Although it was possible to place the electrode very close to the end-plate, as judged by the brief rise times of ACh produced conductance increase, we chose to move the electrode away from the end-plate to reduce the possibility of local ACh concentration fluctuations near the receptor surface which might arise from rapid changes in electrode properties (Katz & Miledi, 1972). Iontophoretic current, supplied through an electro-optical isolation unit connected to a separate bath electrode, was monitored by a differential amplifier mounted near the electrode to insure electrical stability. For some iontophoretic electrodes passage of current was associated with haphazard variations in their resistance; such electrodes were not used. Iontophoretic electrodes had resistances in the range of 10–20 MΩ, and required backing currents of approximately 10 nA.

The voltage clamp was as described earlier (Connor & Stevens, 1971) except that a 60 pF capacitor was placed in parallel with the 1 MΩ feed-back resistor of the current measuring amplifier connected to the bath.

Because we have been concerned in this work with the quantitative comparison of theory and experiment, it has been important to understand the relationship between the actual end-plate currents and the output of our measuring apparatus. We therefore carried out an analysis of our voltage clamping system to calculate the transfer function $\hat{A}(s)$ which relates actual end-plate current $i(t)$ to measured current $I(t)$. For this calculation we assumed that $i(t)$ was injected at a single point into an infinite homogeneous, one-dimensional cable, that membrane potential recording was faithful, that the current passing electrode behaved as an ideal resistor, and that the voltage clamp amplifier had ideal characteristics. This analysis, carried out with standard mathematical techniques (see, for example, Aseltine, 1958), yielded the voltage clamp transfer function

$$\hat{A}(s) \equiv \frac{\hat{I}(s)}{\hat{i}(s)} = 1\Big/\left[1+\frac{R_i}{A\rho}\left(\rho C s+\frac{\rho}{R}\right)^{\frac{1}{2}}\right],$$

where $\hat{i}(s)$ and $\hat{I}(s)$ are the Laplace transforms of the fluctuating e.p.c. and the measured clamp current; (A-1) the voltage clamp amplifier gain; R_i the current passing micro-electrode resistance (Ω); R and C the membrane resistance (Ω cm) and capacitance (F cm^{-1}) per cm of cable length; and ρ the longitudinal resistance of the myoplasm (Ω cm^{-1}). The magnitude squared of the transfer function $|\hat{A}(2i\pi f)|$, a quantity which specifies the over-all frequency response of the voltage clamp-muscle system, is given by

$$|\hat{A}(f)|^2 = \frac{1}{1+\left(\frac{R_i}{A\rho}\right)^2\sqrt{\left\{\left(\frac{\rho}{R}\right)^2+(2\pi\rho Cf)^2\right\}}+\frac{2R_i}{A\rho}\left(\cos\left(\tfrac{1}{2}\tan^{-1}(2\pi R\,Cf)\right)\sqrt[4]{\left\{\left(\frac{\rho}{R}\right)^2+(2\pi\rho Cf)^2\right\}}\right)}.$$

We used amplifier gains A in the range 10^3–10^4, and our current passing electrodes had resistances R_i between 10^6 and 10^7 Ω; these quantities, together with values for the parameters, ρ, R and C (see, for example, Dulhunty & Gage, 1973), permit estimates of the extent to which measured currents are an accurate reflexion of the

actual end-plate currents. Between $f = 1$ and $f = 300$ Hz, the range of frequencies over which spectral densities are reported here, the errors introduced by the voltage clamping equipment (as calculated by the equation above) are at most a few per cent. More detailed calculations, in which properties of the input circuit and voltage clamp amplifier are taken into account, have supported this conclusion.

E.p.c. fluctuations were recorded on magnetic tape (Sanborn, 15 inches/sec; 5 kc band width) simultaneously on a low gain ($\times 5$ to $\times 50$) d.c. channel and on a high gain ($\times 1000$), filtered channel (band pass between 1 and 500 Hz, 40 db/decade rolloff). Typically, at each membrane potential first evoked e.p.c.s were recorded without filtering, then a control sample of current noise without ACh application and spontaneous m.e.p.c.s passed through a 1 kHz low pass filter was taken, and finally the current fluctuations during ACh iontophoresis were recorded.

Estimates of spectral densities (Bendat & Piersol, 1971) were calculated for all fluctuation data from 8,192 digital samples usually taken at 1·02 kHz. A fast Fourier transform routine was used after cosine tapering (Cooley & Tukey, 1965). No filtering was applied to the spectral estimates so as not to obscure possible narrow band width properties of the fluctuations, All data are presented as current spectral density $S(f)$ (A^2 sec *vs.* frequency) and can be directly converted to conductance spectral density $S_g(f)$ by

$$S_g(f) = \frac{S(f)}{(V - V_{eq})^2};$$

V denotes membrane potential and V_{eq} the e.p.c. equilibrium potential.

All calculations including model prediction, rate constant determinations, least-squares regression of voltage dependence and statistical testing were performed on a laboratory digital computer (PDP-11-Digital Equipment).

The most straightforward way to study ACh noise is to record membrane potential fluctuations as Katz & Miledi (1970, 1971, 1972, 1973) have done. The difficulty with this approach is that one is interested in the underlying conductance fluctuations characterized by the conductance spectrum $S_g(f)$, but the measured quantity is the voltage spectrum $S_v(f)$. $S_v(f)$ is not directly proportional to $S_g(f)$ but rather is distorted by the muscle current-to-voltage transfer function $T_M(f)$ according to the relationship (see Stevens, 1972)

$$S_g(f) = \frac{S_v(f)}{|T_M(f)|^2(\bar{V} - V_{eq})^2}.$$

The mean membrane potential is denoted by $\bar{V}$ and it is assumed that voltage fluctuations around this mean are small.

If the muscle transfer function were known, then, the desired quantity $S_g(f)$ could be calculated from the observed $S_v(f)$; in earlier experiments, before the voltage clamp was employed, we adopted such an approach. Unfortunately the simple cable equation and lumped parameter models of muscle cell passive electrical properties are not a sufficiently accurate representation of actual behaviour to permit $T_M(f)$ to be calculated (Falk & Fatt, 1964; Adrian *et al.* 1970). We therefore measured the muscle transfer function in each fibre, at the desired V, by injecting a white noise (flat spectrum) current through a second electrode placed near the end-plate. If the injected current noise spectrum is $\tilde{S}_I(f)$ and the resulting voltage noise spectrum is $\tilde{S}_v(f)$ then the muscle transfer function is given by

$$|T_M(f)|^2 = \tilde{S}_v(f)/\tilde{S}_I(f)$$

and the desired ACh conductance spectrum is obtained from

$$S_g(f) = \frac{S_v(f)\tilde{S}_I(f)}{\tilde{S}_v(f)\,(\bar{V} - V_{eq})^2}.$$

The validity of this method was tested by injecting model synaptic current with known spectrum into a real muscle, then using the voltage response and $|T_M(f)|^2$ to rederive the injected current spectrum. The results demonstrated excellent agreement between the injected and calculated spectra.

The conductance spectra calculated with this technique agreed quantitatively with the voltage clamp records presented later in this paper and provide an independent check on the voltage sensitivity of the ACh noise rate constants. The transfer function method was discontinued in favour of the voltage clamp to permit accurate control of membrane potential over a larger range, and also to eliminate the division of spectra (see equation above) which severely limited accuracy, particularly near the ACh current equilibrium potential.

Frequently used symbols

Symbol	Units	Meaning
T	°C	Temperature of preparation
V	mV	Membrane potential
V_{eq}	mV	Equilibrium potential for end-plate processes
f	Hz	Frequency
μ_g	mho	Mean increase in end-plate* conductance caused by ACh application
μ_I	nA	Mean increase in end-plate* current caused by ACh application
σ_g^2	mho^2	Variance of increase in end-plate* conductance fluctuations caused by ACh application
σ_I^2	nA^2	Variance of increase in end-plate* current fluctuations caused by ACh application
R	Ω cm	Muscle membrane resistance × cm of cable length
C	μF cm^{-1}	Muscle membrane capacitance per cm of cable length
ρ	Ω cm^{-1}	Muscle longitudinal resistance per cm of cable length
R_e	MΩ	Resistance of recording micro-electrode
$S(f)$	A^2 sec	Spectral density at frequency f of membrane current fluctuations
γ	mhos	Conductance of a single two-state ACh channel in its open state
α	msec^{-1}	Rate constant for closing of open ACh channels

* Strictly speaking, 'end-plate' should be replaced by 'muscle' because we have not separated currents flowing through end-plates from those through extrajunctional regions.

RESULTS

Part I. Measurement of ACh produced e.p.c. fluctuations

Current noise in the absence of ACh

Our first objective in this study was to investigate background noise, that is, the extraneous noise arising in our equipment and in the muscle membrane in the absence of ACh; this background noise must be characterized in order to evaluate its contribution to the ACh produced fluctuations which are described in the next section. Briefly, we have found that below about 200 Hz the dominant source is '$1/f$' noise arising in the muscle membrane whereas above 200 Hz, essentially all of the extraneous noise is of instrumental origin. Over the frequency range of interest for the e.p.c. fluctuations to be described later, both the '$1/f$' and instrumental noise were two to four orders of magnitude less than the ACh produced fluctuations we wished to investigate. The reader not concerned with details of our analysis of background noise may omit the remainder of this section without loss of continuity.

In the following presentation, we shall consider first equipment noise and then the '$1/f$' noise arising in the muscle membrane.

After evaluating the possible sources for extraneous noise arising in our measuring apparatus, we discovered that the only significant source was the thermal noise in voltage recording micro-electrode and noise in the first stage of the FET input amplifier. This electrode and amplifier noise is added to the actual membrane voltage and thus acts as a command signal for the voltage clamp system. The current required to clamp the membrane to this noisy signal increases steeply with frequency because the membrane capacitance results in a decreased muscle impedance at high frequencies.

To analyse this effect, we idealized the muscle cell as an infinite one-dimensional cable (Fatt & Katz, 1951) with a thermal noise generator (spectrum $S_v(f) = 4kTR_e$) in the voltage recording electrode resistance (R_e); the mathematical techniques employed in the analysis are those described, for example, by Aseltine (1958). For this system, the spectral density of measured current fluctuations $S_I(f)$ is related to $S_v(f)$ by

$$S_I(f) = S_v(f)\,|T(f)|^2,$$

with $|T(f)|^2$ obtained from the idealized muscle transfer function which is found, with standard techniques (e.g. Aseltine, 1958), to be

$$T(s) = \frac{\hat{I}(0,s)}{\hat{V}(0,s)} = \frac{2}{\rho}(\rho C s + \rho/R)^{\frac{1}{2}}.$$

Here $\hat{I}(0,s)$ and $\hat{V}(0,s)$ are the Laplace transforms of membrane current and voltage at $x = 0$ in the cable and ρ, C, R are longitudinal resistivity (Ω cm^{-1}), membrane capacitance (μF cm^{-1}) and membrane resistance (Ω cm), and the electrode is positioned at $x = 0$; if s is interpreted as imaginary frequency, $T(s)$ is the complex

input impedance of the muscle. Therefore the extraneous thermal contribution to the measured current spectrum $S_I(f)$ is

$$S_I(f) = \frac{4kTR_e(1+2RCf)}{\rho R}. \quad (1)$$

Added to this electrode noise is the extraneous noise contributed by the input stage of the electronics, the principle component being shot noise in the FET input voltage amplifier. This additional amplifier noise may be represented by a thermal noise generator (measured R.M.S. value of 5 μV for our amplifier) of 4 MΩ added to R_e above. The resulting theoretical lower limit for clamp noise resulting solely from recording electrode and amplifier contributions is shown as a continuous curve in Fig. 1; above about 200 Hz the voltage clamp system achieves the minimum possible value.

At low frequencies a membrane potential dependent, '$1/f$' spectrum noise dominates. Such $1/f$ noise in nerve membrane was discovered by Verveen & Derksen at the frog node (1968) and has been observed in lobster axon (Poussart, 1971) and squid axon (Fishman, 1972). Present evidence indicates that $1/f$ noise arises in association with K^+ ion flow in membrane channels. The $1/f$ noise in frog muscle exhibits an equilibrium potential ($V_{eq} = -10$ mV in Fig. 1, $V_{rest} = -50$ mV) which suggests a combination of ionic components. Increases in external K^+ concentration shifted V_{eq} to more positive values implicating this ion in the process, but we have not ruled out the possibility that Na^+ or even Cl^- ions participate in the current which results in a $1/f$ spectrum. $1/f$ noise is not solely a property of the end-plate region but occurs anywhere in frog muscle fibres with or without glycerol treatment. A lumped component model of the muscle studied with our voltage clamp apparatus gave spectra at low frequencies like that shown in Fig. 1 for -10 mV.

In hyperpolarized cells, humps were detected superimposed on the low frequency $1/f$ spectrum. Separation of these components gave a spectrum which seemed to behave as $1/(1+4\pi(f/f_c)^2)$ where f_c depended on membrane potential. Such a case is shown in Fig. 1 (-80 and -120 mV). Records were sorted to ensure that no spontaneous m.e.p.c.s were present. It is possible that these humps are spectra of current fluctuations in Hodgkin–Huxley type K^+ channels (Siebenga & Verveen, 1972; Stevens, 1972; Fishman, 1973).

In summary, all the extraneous noise added by the electrodes, voltage clamp and associated electronics has been quantitatively accounted for and under the conditions of our experiments these sources limit the resolution to about 1×10^{-12} A $(\text{sec})^{\frac{1}{2}}$ at 100 Hz. ACh induced current fluctuations reported below are generally three orders of magnitude above these extraneous background sources.

In order to minimize contributions from background noise, control spectra (obtained in the absence of ACh) have always been subtracted from the

e.p.c. spectra presented in succeeding sections. Since the extraneous noise varies in magnitude with membrane potential (see Fig. 1), it was necessary to obtain a control spectrum for each membrane potential used. This subtraction procedure is justified because the extraneous sources should be uncorrelated with the ACh fluctuations we wished to study. In practically all cases the correction amounted to at most a few per cent.

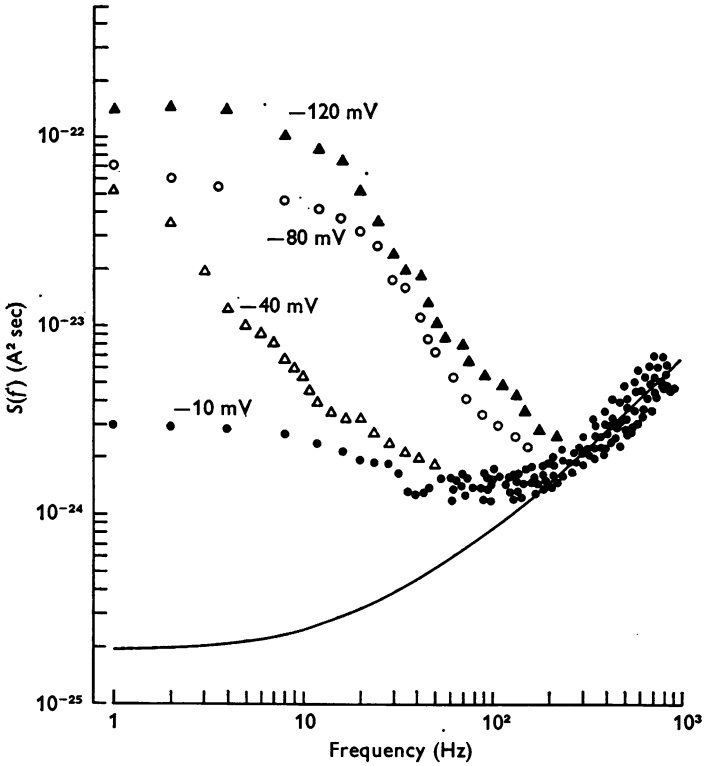

Fig. 1. Current fluctuation spectral densities from voltage clamped endplate in an ethylene glycol treated muscle at 10° C without ACh. Membrane potential is shown with each curve. Continuous line represents the contributions from thermal and amplifier noise (eqn. (1)) calculated for the observed R_e = 3 MΩ, input resistance = 0·45 MΩ, fibre radius = 50 μm and using longitudinal resistivity = 200 Ω cm (Falk & Fatt, 1964), $C_M = 2\mu F/cm^2$ (Gage & Eisenberg, 1969, Table 1). $1/f$ noise present in the input amplifier was not included in this calculation; addition of this component would result in a spectrum similar to the observed one shown above for $V = -10$ mV. Note the $1/f$ component visible at low frequencies and the humps apparent in records taken at large hyperpolarizations.

Membrane current fluctuations produced by ACh

Fig. 2 demonstrates the result of iontophoretic application of ACh to a voltage clamped end-plate. The mean end-plate current increases (lower traces) and is accompanied by a marked increase in the current noise variance, shown at high gain on the top traces; a spontaneous miniature end-plate current is shown in the control record for comparison.

If mean e.p.c. is varied by altering the ACh concentration, the magnitude of the current fluctuations is found to vary as well. We have examined this

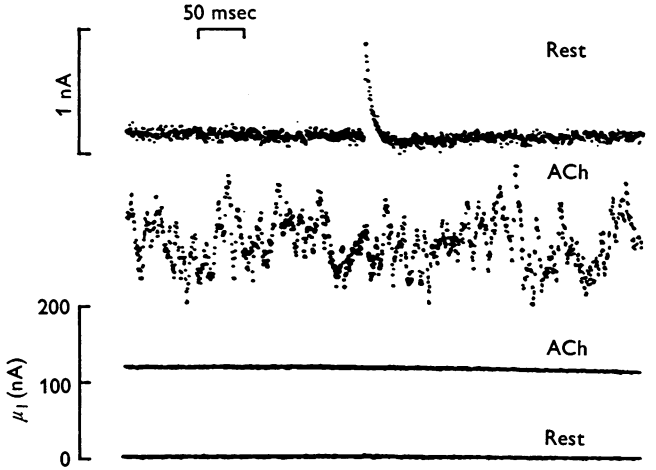

Fig. 2. Digitalized time sweep of membrane currents in voltage clamped end-plate of ethylene glycol treated muscle at 8° C. High gain, records filter below 1 Hz (40 db/decade) are presented above and low gain d.c. coupled traces below. The control trace includes a spontaneous miniature end-plate current. Iontophoretic application of ACh[current = 10 nA] produced a mean end-plate current of 120 nA and increase in R.M.S. noise from 0·07 to 0·25 nA (measured with 500 Hz, low pass active filter). The upper two traces are shown on the same scale. $V = -100$ mV.

relation by measuring the mean (μ_I) and variance (σ_I^2) of e.p.c.s. Because the various records were taken at a variety of driving potentials (membrane potential V *minus* equilibrium potential V_{eq}), we have expressed this relation between mean and variance in terms of membrane conductance by using the following equations which result directly from Ohm's law:

$$\mu_g = \frac{\mu_I}{(V - V_{eq})}, \quad \sigma_g^2 = \frac{\sigma_{I^2}}{(V - V_{eq})^2}.$$

Fig. 3 presents a graph of conductance variance σ_g^2 as a function of mean end-plate conductance μ_g for ACh noise obtained in three experiments. In

these and additional experiments conductance variance was linearly related to mean conductance by (eqn. (20) in Stevens, 1972)

$$\sigma_g^2 = \gamma \mu_g, \tag{2}$$

where the proportionality γ has a value of $0{\cdot}205 \pm 0{\cdot}0063$ (S.E.) $\times 10^{-10}$ mho. According to the interpretation we have placed on the e.p.c. fluctuations (see p. 668), γ is the conductance of a single open end-plate channel.

The conductance fluctuations shown in Figs. 2 and 3 are the basis of the ACh voltage noise first studied by Katz & Miledi (1971, 1972).

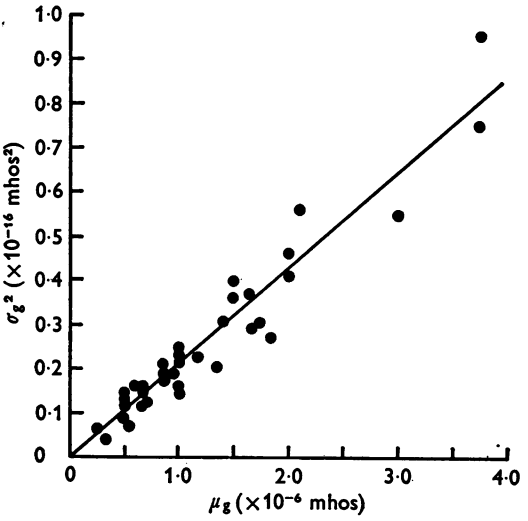

Fig. 3. Variance of conductance fluctuations as a function of mean end-plate conductance increase produced by iontophoretic application of ACh. Data were pooled from three experiments, and points were taken at a variety of membrane potentials between 60 and -140 mV. Slope of the relationship gives the conductance of a single channel (see eqn. (2)) and has a value of $0{\cdot}19 \times 10^{-10}$ mho for the three experiments shown here. The value from eighty-four estimations in eight experiments was $0{\cdot}205 \pm 0{\cdot}0063$ (S.E.) $\times 10^{-10}$ mho.

Spectrum of ACh produced e.p.c. fluctuations

The properties of the ACh induced fluctuations were characterized by spectral densities calculated from digitalized records of e.p.c. taken before significant desensitization had occurred. All of the over 200 e.p.c. spectra calculated for more than 40 voltage clamped end-plates had the same form: spectral densities were constant at low frequencies and approached $1/f^2$ at high frequencies. Examples of typical e.p.c. spectra are illustrated in Figs. 4, 5 and 10.

The fast Fourier transform yields spectral estimates $S(f)$ that are distributed according to χ^2 distribution with standard deviation

$$\sigma = \{VAR(S(f))\}^{\frac{1}{2}} = S(f)/B_e T = 0{\cdot}2\, S(f)$$

(Bendat & Piersol, 1971); our calculations used a resolution band width $B_e = 3$ cycles and record length $T = 8{\cdot}192$ sec or 3192 samples. The error bars on each power spectrum indicate ± 1 S.D. ($\pm 1\sigma$).

Desensitization does not affect the form of $S(f)$

During a constant iontophoretic pulse of ACh the post-synaptic depolarization gradually diminishes (Katz & Thesleff, 1957). We have standardly observed this desensitization under voltage clamp and have selected for analysis e.p.c. records early in ACh current plateau before the mean current decreased appreciably. Since the mechanism of desensitization is poorly understood, we also compared e.p.c. spectra calculated from noise samples taken before appreciable desensitization occurred and during the various levels of desensitization produced by continuous application of ACh. As desensitization progressed, the mean current μ_I diminished, and there was a concomitant decrease in the noise amplitude as measured by $S(O)$ or σ_I^2; throughout, however, σ_I^2 was linearly related to μ_I with the same proportionality constant that characterized this relationship at undesensitized end-plates. Although the magnitude of the spectra decreased, the spectral shape and cut-off frequency (that frequency for which the spectral density if one half of the zero frequency asymptote) remained constant for from 0 to 90% desensitization. We have also noticed that desensitization occurred more rapidly in hyperpolarized cells (Magazanik & Vyskočil, 1970).

Part II. Interpretation of e.p.c. fluctuations

In the preceding Part, we have characterized the background noise current measured in voltage clamped muscle cells and have shown that this extraneous noise does not generally make an appreciable contribution to the comparatively large e.p.c. fluctuations caused by ACh application. Further we have found that the amplitude of ACh produced conductance fluctuations, as measured by their variance, is proportional to the mean end-plate conductance, that the spectrum of conductance fluctuations is constant at low frequencies and declines as does $1/f^2$ in the high-frequency limit, and that the form of this spectrum is not affected by desensitization. To interpret these observations in terms of end-plate conductance mechanisms, some theory about the source of the fluctuations is required. In this section we first develop a theoretical framework which relates e.p.c. spectra to post-junctional events, and then test the adequacy of this theory by comparing a number of predictions about the behaviour of e.p.c. fluctuations with experimental observations.

Model for interpreting noise structure

On the basis of recent experiments (Magleby & Stevens, 1972*a*, *b*), a quantitative model for the kinetics of channel opening and closing has been proposed and shown to describe accurately the time course of the end-plate permeability increase which follows nerve stimulation. According to this view, ACh combines with the receptor molecule, and the receptor–ACh complex undergoes a conformational change analogous to that seen in enzyme-substrate systems (see Eigen & Hammes, 1963; Hammes, 1968*a*, *b*; Gutfreund, 1971; and references cited in Chock, 1971). This model was developed for a situation in which the post-junctional membrane is subjected to brief transient increases in ACh concentration, but it also makes predictions about the statistical structure of the fluctuations observed when the post-junctional membrane is subjected to a constant ACh concentration (see Magleby & Stevens, 1972*b*; Stevens, 1972).

With a constant ACh concentration and very rapid binding of ACh to its receptors (cf. Eigen & Hammes, 1963), the ACh-receptor complexes are viewed as continually fluctuating between the 'open' and 'closed' conformations (see Magleby & Stevens, 1972*b*; Katz & Miledi, 1972):

$$nT + R \underset{}{\overset{K}{\leftrightarrows}} T_n R \underset{\alpha}{\overset{\beta}{\leftrightarrows}} T_n R^*. \tag{3}$$

Here T denotes ACh, R receptor, TR and TR^* the 'closed' and 'open' conformations of the complexes, and n ACh molecules per channel are assumed necessary for a channel to open; K is the binding constant of ACh and its receptor, and α and β are the indicated rate constants. The rapid opening and closing of end-plate channels, which we view as the source of the ACh produced e.p.c. fluctuations, are thus governed by the binding constant K, and the rate constants α and β.

The key to our analysis, then, is that these same rate constants (in eqn. (3)) are reflected both in e.p.c. fluctuations produced by the iontophoretic application of ACh, and in the kinetics of nerve-evoked e.p.c.s. Our theory may therefore be tested not only by evaluating the accuracy of the equation for e.p.c. spectra (see eqn. (4) below) derived from our picture of post-junctional events, but more critically by investigating predictions (described below) about relations between e.p.c. spectra and properties of the end-plate conductance changes produced by axonal ACh release.

In the remainder of this Part we present five tests of the theory just described; these tests are based on equations derived in the Appendix and in Magleby & Stevens (1972*b*). Note that the various tests outlined below are not all independent, but that they have been separated into five distinct categories to aid in the presentation of experimental results.

(i) *The spectrum $S(f)$ of ACh produced e.p.c. fluctuations is given by*

$$S(f) = \frac{2\gamma\mu_I(V - V_{eq})/\alpha}{1 + (2\pi f/\alpha)^2}. \quad (4)$$

Here $S(f)$ is the spectral density at frequency f, μ_I is the mean e.p.c., V is the membrane potential, V_{eq} is the end-plate equilibrium potential, α is the rate constant for channel closing (from eqn. (3)) and γ is the conductance of one open channel. Note that this equation holds exactly, because of restrictions in its derivation (see Appendix), for the limit of low ACh concentrations. The meaning of 'low ACh concentrations' and the accuracy of this assumption for our experiments is considered in the Discussion.

The cut-off frequency f_c of the spectrum $S(f)$ above is defined to be $f_c = \alpha/2\pi$ and is that frequency at which $S(f)$ has decreased to half of its zero frequency asymptote. Magleby & Stevens (1972*b*) have predicted that α should depend exponentially on membrane potential according to the relation

$$\alpha = Be^{AV} \quad (5)$$

and have shown that α, as estimated from nerve-evoked e.p.c.s, does indeed conform to this prediction. In terms of this analysis, the constant A reflects a dipole moment change associated with the conformational transition of the end-plate channel gating molecule from 'open' to 'closed', and the constant B is related to the free energy barrier for this conformational change in the absence of a perturbing membrane electric field. Because the cut-off frequency (that is, the half-amplitude frequency) may be conveniently measured from the ACh spectra, these spectra provide, through the relation $f_c = \alpha/2\pi$, a means of estimating α. As a consequence of eqns. (4) and (5), (ii) *estimates of α obtained from e.p.c. spectra should depend exponentially on membrane potential.*

According to the development by Magleby & Stevens (1972*b*) and that presented here (Appendix) α may be estimated in three ways: (*a*) as the decay constant of nerve-evoked e.p.c.s, (*b*) as the decay constant for m.e.p.c.s, and (*c*) from the cut-off frequency of ACh produced e.p.c. spectra. Estimates of α by these three means will be distinguished by subscripts as α_e (from nerve-evoked e.p.c.s), α_m (from m.e.p.c.) and α_a (from e.p.c. spectra). If our theory is correct, then, (iii) *estimates of α by these three means should coincide.* Thus, for a given end-plate semilogarithmic plots of α_e, α_m, and α_a as a function of membrane potential should all cluster around the same straight line (see eqn. (5)).

The parameter α_e has a membrane potential dependent Q_{10} of approximately 3; more specifically, A of eqn. (5) increases with lower temperatures (Magleby & Stevens, 1972*b*). Accordingly, (iv) the Q_{10} of α_a *should be about 3 and should vary with membrane potential.*

The parameter γ in eqn. (4) is, in our analysis, the conductance of one open channel. Magelby & Stevens (1972*b*) have presented evidence that end-plate channel conductance is independent of membrane potential, that is, that end-plate channels do not show appreciable rectification. This observation implies that (v) *the parameter γ in eqn. (4) should have the same value when estimated from spectra obtained at various membrane potentials.*

The succeeding sections deal, in turn, with these predictions.

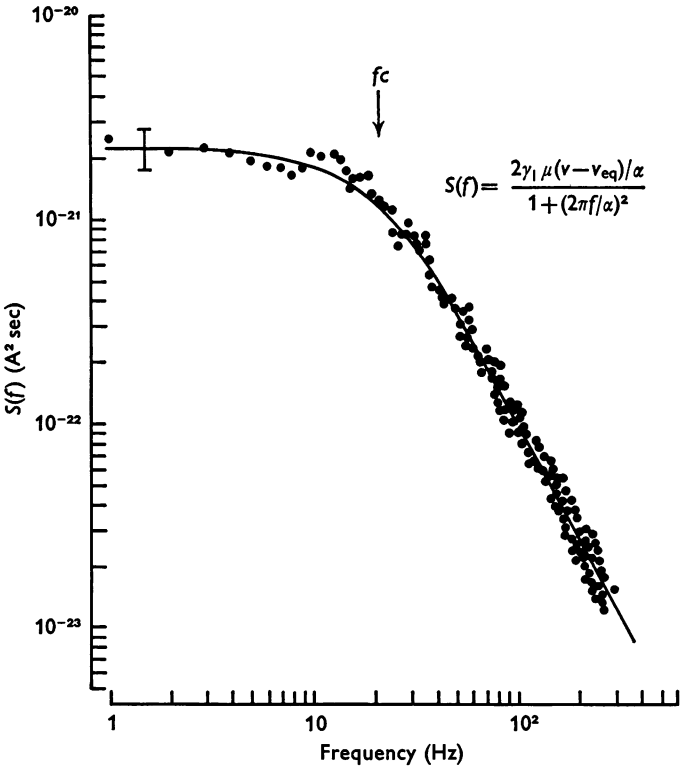

Fig. 4. Spectral density of e.p.c. fluctuations produced by a constant ACh iontophoretic application to a voltage-clamped ethylene glycol treated muscle end-plate. $V = -60$ mV, at 8° C. The continuous line is the theoretical spectrum calculated from the model presented in the text (eqn. (4)) using the measured mean current ($\mu_I = 80 \times 10^{-9}$ A), equilibrium potential ($V_{eq} = 0$), $\alpha = 0{\cdot}132$ msec^{-1}, and assuming a single channel conductance $\gamma = 0{\cdot}32 \times 10^{-10}$ mhos. The cut-off frequency $f_c = \alpha_a/2\pi =$ 21 HZ is indicated by an arrow. The error bar indicates $\pm 1\sigma$. The spectrum is based on 8192 digital samples taken at 1·02 kHz through a 300 Hz active low pass filter. This plot can be converted to a conductance fluctuation spectrum (units: mho^2-sec) by multiplying ordinate values by $1/(0{\cdot}06)^2$.

Equation (4) accurately describes e.p.c. spectra

Specimen e.p.c. spectra for various membrane potentials and temperatures are presented in Figs. 4, 5 and 10 with smooth curves calculated from eqn. (4) superimposed upon the experimentally determined estimates of spectral density. Although the experimental points scatter somewhat about the theoretical curves, the extent of this scatter is no larger than

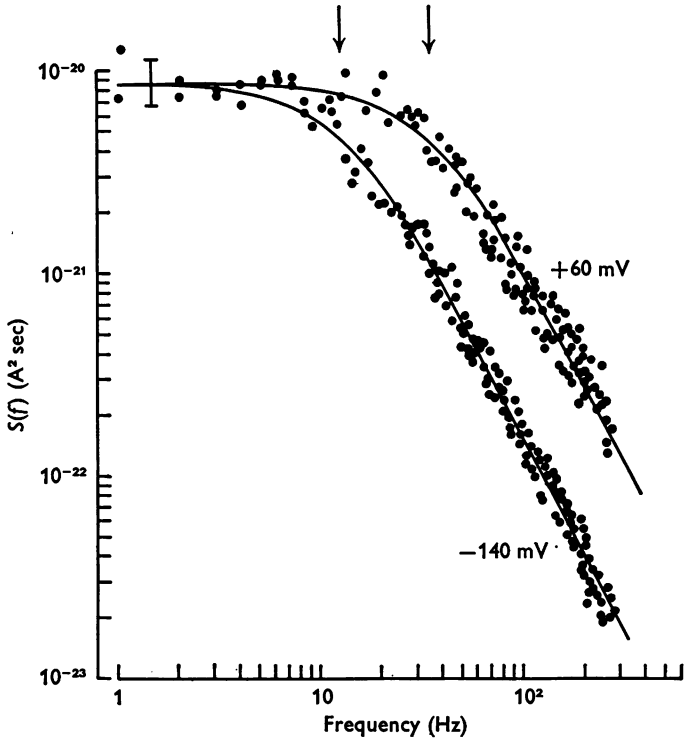

Fig. 5. Effect of membrane potential on the ACh induced e.p.c. fluctuation spectrum. Ethylene glycol treated muscle at 8° C for $V = -140$ and $+60$ mV. Vertical axis as labelled applies to the -140 mV curve. The $+60$ mV curve has been shifted along the vertical axis to facilitate comparison with the -140 mV curve; multiply ordinate values by 8×10^{-3} to obtain spectral densities (A^2 sec) for the $+60$ mV curve. Error bar indicates $\pm 1\sigma$. Continuous curves are predicted spectra from the model in the text (eq. (4)), using the following parameters: $V_{eq} = 0$; for $V = +60$ mV curve, $\alpha = 0{\cdot}214$ msec^{-1}, $\mu_I = -5 \times 10^{-9}$ A, $\gamma = 0{\cdot}24 \times 10^{-10}$ mhos; for $V = -140$ mV curve, $\alpha = 0{\cdot}075$ msec^{-1}, $\mu_I = 90$ nA, $\gamma = 0{\cdot}30 \times 10^{-10}$ mho. The cut-off frequencies $f_c = \alpha_a/2\pi$ indicated by arrows are 12 Hz (-140 mV) and 34 Hz ($+60$ mV). Conversion to conductance spectra (units: mho^2 sec) can be made by multiplying the appropriate ordinate values by $(1/0{\cdot}14)^2$. Direct comparison can be made to Fig. 4 taken from the same cell.

expected by the statistical uncertainty in the spectral estimates as indicated by the error bars in the Figures. Eqn. (4) has been found to provide an adequate fit to the experimental data for all e.p.c. spectra we have measured.

The cut-off frequency of e.p.c. spectra depends exponentially on voltage

The effect of membrane potential on the ACh produced e.p.c. spectrum is demonstrated in Fig. 5. The shape of the spectra are the same for various membrane potentials, differing only by a simple displacement along the frequency axis: hyperpolarization results in a lower cut-off frequency. In terms of our physical picture, hyperpolarization causes a slower relaxation of the conformation change associated with channel closing.

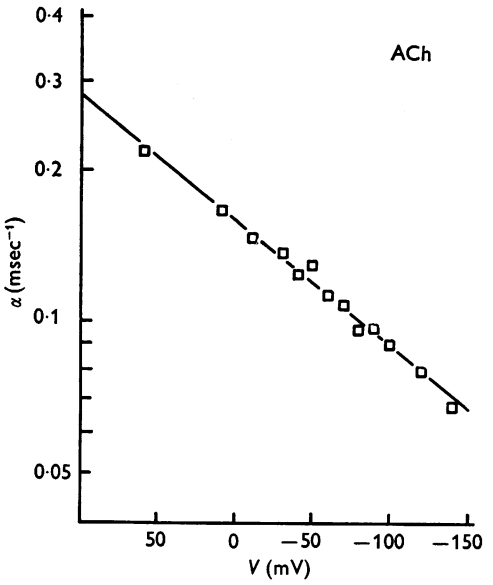

Fig. 6. Semilogarithmic plot of rate constants ($msec^{-1}$) calculated from cut-off frequencies ($f_c = \alpha_a/2\pi$) of ACh induced fluctuation spectra at various membrane potentials. Data is from a single end-plate at 8° C in an ethylene glycol treated muscle. Solid line is a least squares fit corresponding to $\alpha = Be^{AV}$ (eqn. (5)) with $A = 0{\cdot}0059\ mV^{-1}$ and $B = 0{\cdot}17\ msec^{-1}$.

The rate constant $\alpha_a = 2\pi f_c$ ($msec^{-1}$) determined from these spectra was found to depend exponentially on V as shown on a semilogarithmic plot in Fig. 6. To obtain each point in Fig. 6 spectral estimates for e.p.c. fluctuations were fitted by eqn. (4) and the corresponding α_a determined from the cut-off frequency f_c. The least squares line shown in Fig. 6 is precisely the dependence predicted by eqn. (5). A and B of (5) exhibited

some variation between different preparation; for thirteen end-plates mean values were (T between 8 and 11·5° C) $\bar{A} = 0{\cdot}0058 \pm 0{\cdot}008\ \text{mV}^{-1}$ and $\bar{B} = 0{\cdot}24 \pm 0{\cdot}015\ \text{msec}^{-1}$.

All estimates of α coincide

Magleby & Stevens (1972*a*, *b*) studied the voltage dependence of nerve-evoked e.p.c. kinetics and Gage & McBurney (1972) have carried out a similar investigation of m.e.p.c.s; e.p.c. and m.e.p.c. properties have not however, been studied simultaneously so that a direct comparison could

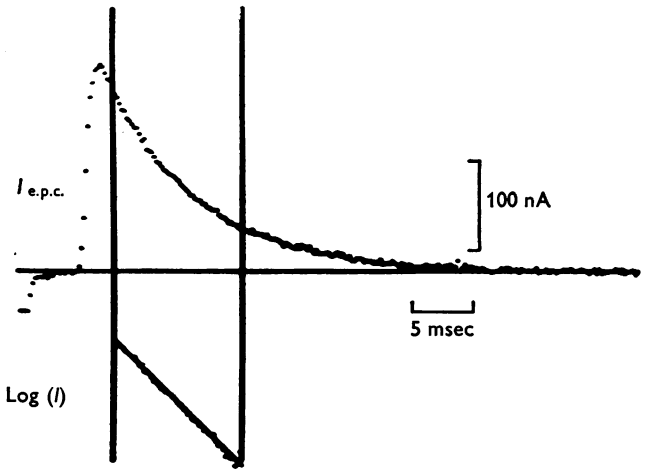

Fig. 7. Digitalized nerve-evoked e.p.c. recorded in voltage clamped end-plate of an ethylene glycol treated muscle at $V = -50$ mV and 8° C. Base line drawn as average of last 2 msec of the record. Decay phase between the vertical cursors is plotted below on semilogarithmic co-ordinates. Continuous line through these points is a least squares fit.

be made. Since our model predicts that the decay constant α_e for nerve-evoked e.p.c.s and α_m for spontaneous m.e.p.c.s should have the same values, the following procedure was adopted to test this prediction and to compare α_m and α_e with the values of α_a obtained from e.p.c. spectra. At each V evoked e.p.c.s, m.e.p.c.s, and ACh produced e.p.c. fluctuations were recorded. The e.p.c. spectrum was calculated and fitted with the theoretical (eqn. (4)) using both γ and α as free parameters. From this, graphs of α_a *vs.* V were obtained as in Fig. 6. Then e.p.c. and m.e.p.c. decay rate constants α_e and α_m were determined and their dependence on V compared to that of α_a.

As expected from recent work, e.p.c.s decay exponentially (Magleby & Stevens, 1972*a*; Kordas, 1972*a*, *b*). Fig. 7 shows a digitalized e.p.c. and

semilogarithmic plot of the decaying phase; the superimposed least squares line, conforming to the prediction of the model (Magleby & Stevens, 1972*b*), obscures most of the points. The e.p.c. decay constants, determined from the slopes of these semilogarithmic plots, are shown in Fig. 9*A* for various V. As expected the variance of α estimates increased somewhat near the equilibrium potential, where the currents were small, but in all cases the results were entirely reproducible.

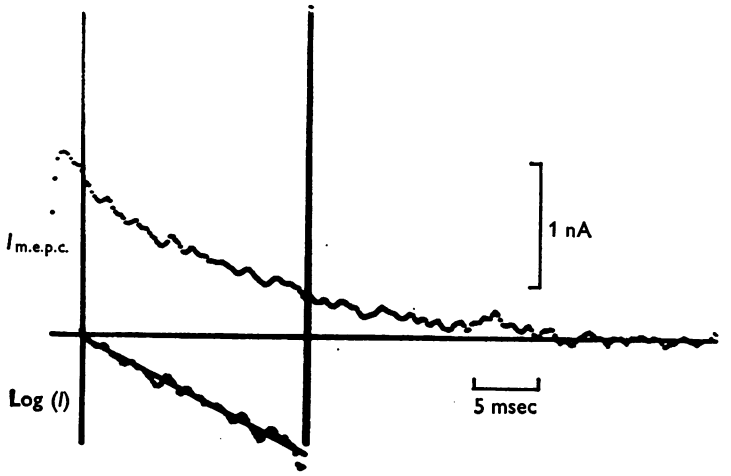

Fig. 8. Digitalized record of a spontaneous m.e.p.c. recorded in a voltage clamped, ethylene glycol treated muscle at $V = -120$ mV and 8° C. Below is a semilogarithmic plot of the decay phase of the m.e.p.c. between the vertical cursors. The straight line through these points is fitted by the least square method from the form $I(t) = I(0)\,e^{-\alpha t}$. The base line is calculated as the average of the final 2 msec of the current trace.

The declining phase of m.e.p.c.s follows the same exponential course as that just described for e.p.c.s. The low noise levels of the voltage clamp permitted relatively accurate determination of the exponential decay of the m.e.p.c. tails as shown in Fig. 8. Similar observations have also been made by Gage & McBurney (1972). Like the decay constant of e.p.c.s, the voltage dependence of α_m is clearly exponential over the whole range of membrane potentials used (-140 to 60 mV) as demonstrated by the data in Fig. 9*B*). The same end-plate gave the data for Fig. 9*A* and *B*; the least squares line fit in Fig. 9*A* is drawn on Fig. 9*B* for comparison. Because of the somewhat less favourable signal to noise ratio for m.e.p.c.s, the values of α_m scatter somewhat more around least squares line than those of α_e.

A composite plot of rate constants α_a, α_e, and α_m determined from e.p.c. fluctuations, nerve-evoked e.p.c.s and spontaneous m.e.p.c.s measured at the same end-plate under the same conditions is given in Fig. 9*C*. The

least squares lines for each set of estimates do not differ significantly from the collective regression line by a Student's t test ($P < 0{\cdot}05$). This line may be used to predict the closing rate of open ACh controlled ionic channels at any membrane potential (eqn. (5)). It should be emphasized that the estimates of α_a from ACh produced fluctuations are completely independent of α_e and α_m calculated from e.p.c.s and m.e.p.c.s, and all α estimates are made without the use of free parameters.

Temperature dependence of $S(f)$

Increasing temperature shifts the e.p.c. spectrum toward higher frequencies without otherwise altering its shape (Katz & Miledi, 1972). We have confirmed these observations as shown in Fig. 10 for 8 and 18° C taken at the same end-plate at -70 mV. The model presented earlier predicts this temperature dependence of the rate constants based upon the temperature sensitivity of the transition energy for the conformation change associated with the ionic gating mechanism. Curves calculated from eqn. (4) using a Q_{10} for α_a of 2·77 are shown in Fig. 10 as continuous lines.

The logarithm of α_a continues to depend linearly on membrane potential at higher temperatures (Fig. 11) but exhibits a decreased slope similar to that reported for e.p.c. tails (Magleby & Stevens, 1972*b*). The Q_{10} is therefore membrane potential dependent and varied in Fig. 11 from 2·4 at -50 mV 3·6 at -100 mV.

Conductance of a single channel

In order to minimize the minor influences of variability in α_a estimates on the measurement of single channel conductance γ, e.p.c. spectra were refitted by eqn. (4) using regression values for α_e from the same end-plate. This procedure, performed with the aid of the computer, involved varying the single free parameter γ by vertically shifting the theoretical curve (eqn. (4); see Fig. 3) until good visual agreement between the curve and spectral estimates was attained. The conductance of a single channel, γ, was then calculated from eqn. (4) at $f = 0$:

$$\gamma = \frac{S(O)\alpha}{2\mu_I(V - V_{eq})}. \tag{6}$$

A histogram of twenty γ estimates taken at a single end-plate is shown in Fig. 12. The mean conductance $\bar{\gamma} = 0{\cdot}32 \pm 0{\cdot}009$ (S.E.) $\times 10^{-10}$ mhos is somewhat higher than the grand mean of estimates from eight experiments which gave $\bar{\gamma} = 0{\cdot}205 \pm 0{\cdot}0063 \times 10^{-10}$ mhos ($n = 84$). This experiment was chosen for presentation because the voltage clamp of the end-plate was unusually good (see Methods for criteria) and produced large γ estimates. In an imperfectly voltage clamped cable-like structure, the space

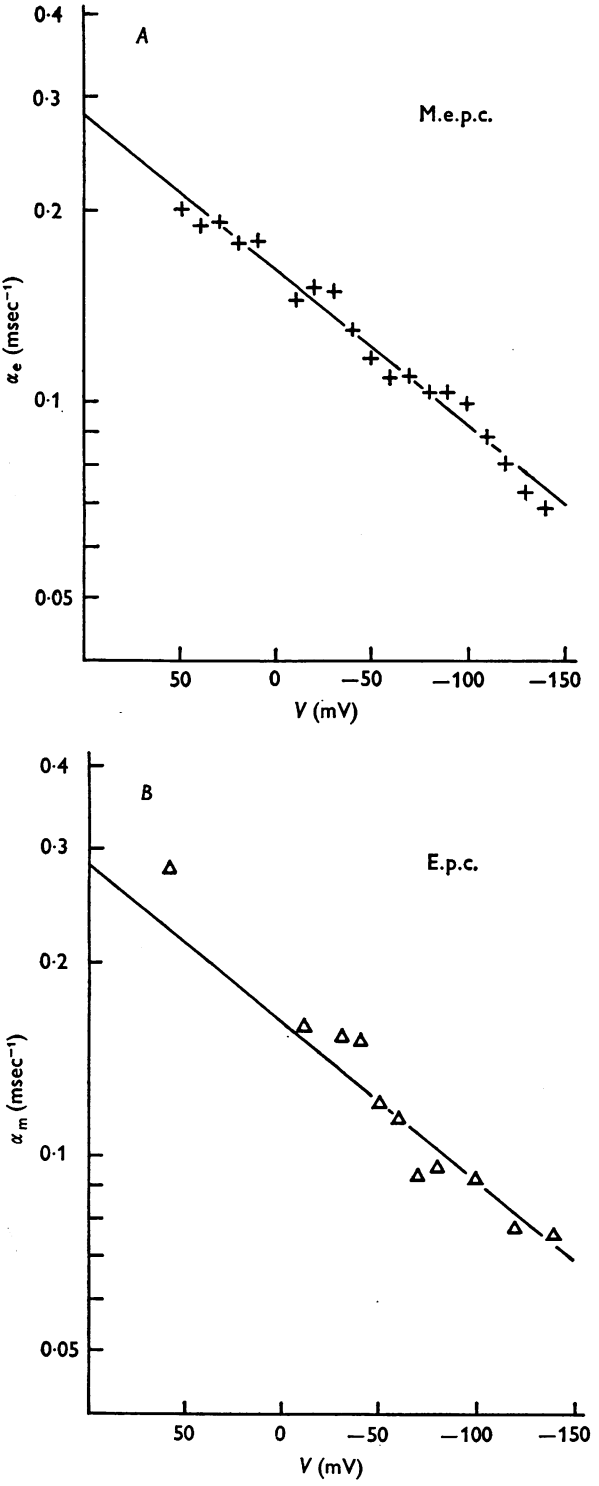

Fig. 9*A* and *B*. For legend see facing page.

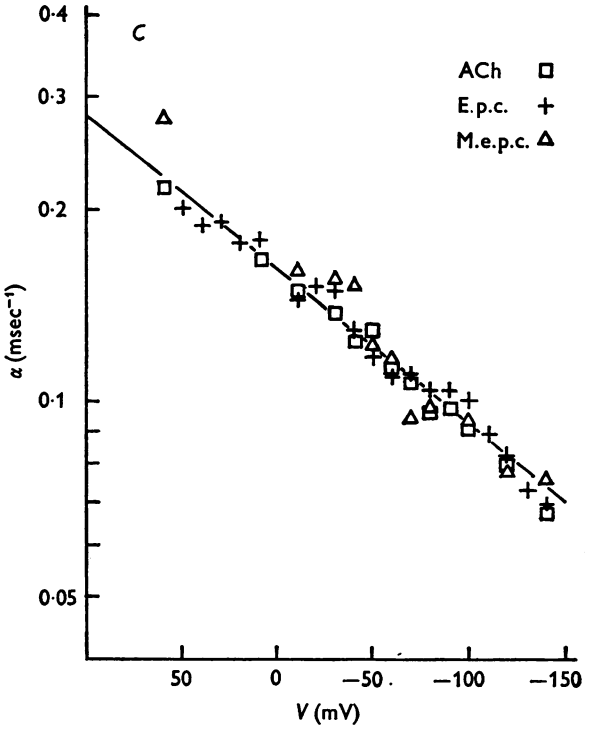

Fig. 9. *A*, semilogarithmic plot of end-plate current decay rate constant α_e (msec^{-1}) *vs.* membrane potential *V*. Data taken from a voltage clamped end-plate in an ethylene glycol treated muscle at 8° C. Continuous line is the least squares fit of the form $\alpha = Be^{AV}$ (eqn. (5)) where $A = 0{\cdot}0059$ mV^{-1} and $B = 0{\cdot}17$ msec^{-1}. *B*, semilogarithmic plot of the rate constants α_m of the decays of spontaneous m.e.p.c.s recorded from the end-plate of *A*. The continuous line is reproduced from *A*. *C*, semilogarithmic plot of rate constants for ACh channel closing *vs.* membrane potential. Data is superimposed from Figs. 6 and 9*A*, *B*. E.p.c. fluctuations, evoked e.p.c.s and spontaneous m.e.p.c.s were recorded at each membrane potential before changing *V*. Data were taken first from 0 to −140 mV at steps of −20 mV then back to 0 at odd multiples of 10. Finally the points from 0 to +60 MV were recorded. The complete run required 20 min. The equilibrium potentials of e.p.c.s and m.e.p.c.s were repeatedly checked during the run to insure stability. The least square line is drawn from the form $\alpha = Ae^{BV}$ (eqn. (5)) where $A = 0{\cdot}0059$ mV^{-1} and $B = 0{\cdot}17$ msec^{-1}. The least squares lines for the individual sets of points do not differ significantly from the mean according to a *t* test ($P < 0{\cdot}05$).

constant is a function of frequency ($\lambda(f)$) and will appear longer for d.c. than for fluctuating currents, an effect which tends to produce underestimates of $S(O)/\mu_I$ as well as low pass filtering $S(f)$, thereby reducing the apparent α_a. In addition, more positive estimates of the equilibrium

potential would result if voltage control were less than ideal. Altogether then, if some portions of the end-plate are electrically remote from the clamping electrodes, γ will be underestimated. We emphasize, however, that the possibility of genuine differences between the open single channel conductances of different muscles must be considered.

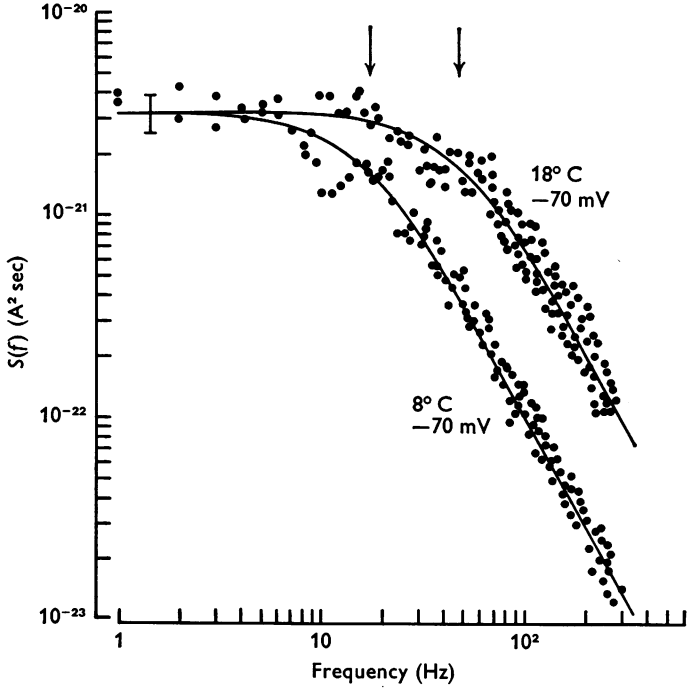

Fig. 10. Effect of temperature on the e.p.c. fluctuation spectrum at constant membrane potential $V = -70$ mV. Records for 8 and 18° C are shown. Ordinate applies to 8° C curve and should be multiplied by 0·36 for the 18° C spectrum. The continuous curves are predicted from eqn. (4) with the cut-off frequencies f_c shown by arrows. ($f_c(-70$ mV, 8° C) = 17·9 Hz, $f_c(-70$ mV, 18° C) = 49·2 Hz), giving a Q_{10} of 2·77. The error bar shows $\pm 1\sigma$ for the spectral estimates. $\mu_I = 100 \times 10^{-9}$ A at both temperatures. Recorded from voltage clamped end-plate after treatment with ethylene glycol. Multiply ordinate values by $(1/0{\cdot}07)^2$ to convert conductance spectral densities (mho² sec).

The spread of γ values about the mean seems attributable entirely to the variances associated with measurements of μ_I, $S(O)$, α_a and $(V-V_{eq})$. The largest error was associated with estimates of the mean current μ_I (10 %) and $S(O)$ ($\pm$ 10 %). Rate constants predicted from e.p.c.s showed very little variance ($<$ 1 %) as did $(V-V_{eq})$ which was subject primarily to systematic errors through inaccuracy in V_{eq} ($\pm$ 5 mV).

Integration of the ACh noise spectrum over frequency gives the total fluctuation variance

$$\sigma_I^2 = \int_0^\infty S(f)\,df.$$

Substitution from eqn. (4) into this expression yields

$$\sigma_I^2 = \gamma\mu_I(V - V_{eq})$$

which provides another means of estimating γ that does not require computing e.p.c. spectra. An R.M.S. meter was used for this measurement and produced results in excellent agreement with data presented in Fig. 12.

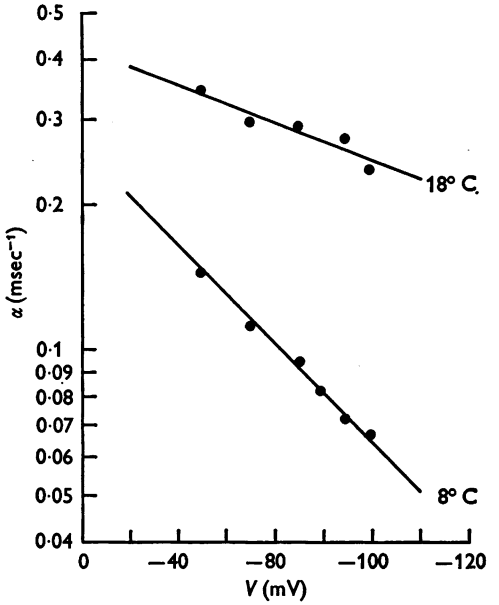

Fig. 11. Semilogarithmic plot of the rate constants α_a calculated from the cut-off frequencies of e.p.c. spectra *vs.* membrane potential at two temperatures 8 and 18° C. Solid lines are least squares fits using $\alpha = Be^{AV}$ (eqn. (5)): $A_{8°C} = 0{\cdot}015\ \text{mV}^{-1}$, $B_{8°C} = 0{\cdot}26\ \text{msec}^{-1}$. $A_{8°C} = 0{\cdot}0057\ \text{mV}^{-1}$, $B_{18°C} = 0{\cdot}42\ \text{msec}^{-1}$. The slopes are significantly different (t test: $P < 0{\cdot}05$).

Estimates of the single channel open conductance were not demonstrably dependent upon membrane potential, mean end-plate current or rate constant α_a. Least squares lines fitted to these relations had slopes which did not significantly differ from zero (t test, $P < 0{\cdot}001$). The variance about these least squares lines was large enough, however, to obscure possible weak relationship between single channel conductance and V, μ_I or α_a.

The effect of temperature on γ is shown in Fig. 13. The mean and $\pm 1\sigma$ are depicted for all experiments pooled at each temperature. No statistically significant ($P < 0{\cdot}01$) dependence of γ on temperature was observed in these experiments, although scatter in γ estimates was sufficient to obscure a $Q_{10} = 1{\cdot}2$ or $1{\cdot}3$ such as has been observed for $\bar{P}_K$ and $\bar{P}_{Na}$ in frog node (Frankenhaeuser & Moore, 1963).

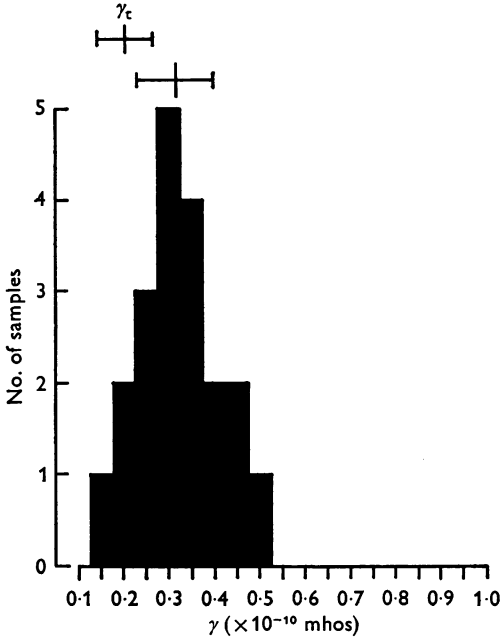

Fig. 12. Histogram of the conductance of individual open ACh channels from one end-plate. Single channel conductance γ is calculated from the low frequency asymptotes of the e.p.c. fluctuation spectra fit using the cut-off frequency predicted from the continuous line in Fig. 9*C* according to eqn. (6). Mean $\gamma = 0{\cdot}32 \pm 0{\cdot}009$ (S.E.) $\times 10^{-10}$ mhos and bar depicting $\pm 1\sigma$ is shown. The grand mean $\bar{\gamma} = 0{\cdot}205 \pm 0{\cdot}0063$ (S.E.) $\times 10^{-10}$ mhos is shown above with a bar over $\pm 1\sigma$. The grand mean is based on eighty-four estimates from eight end-plates each, of which were analysed over a wide range of membrane potentials.

DISCUSSION

Inferences about mechanisms from fluctuation phenomena depend upon assumptions about a system's physical properties, and we have analysed our data within a particular theoretical framework. The most general statement that we can make about our results, however, without recourse to any particular theory of end-plate function, is that a fluctuation–dissipation theorem (Kubo, 1957) applies to the post-junctional membrane

response to ACh. More specifically, the spectrum of end-plate conductance fluctuations may be calculated from the decay of end-plate currents by a Fourier transform. What this means in physiological terms is that the same mechanisms, whatever they are, underlie both the decay of end-plate currents and the ACh produced conductance fluctuations. Thus the kinetics of the end-plate response to ACh may, indeed, be studied by investigating the statistical structure of fluctuations around equilibrium.

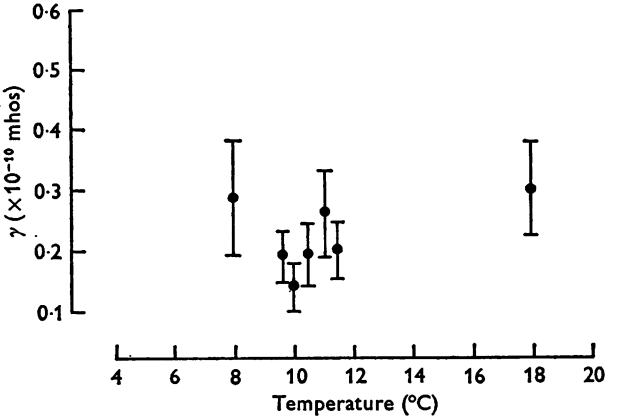

Fig. 13. Dependence of single channel conductance estimates γ on temperature. Data are pooled for all experiments at each temperature. The γ values are from eighty-four estimates in eight end-plates. The bars represent $\pm$ 1 S.D. A least squares line fit to these data gave a Q_{10} which was not significantly different than 1·0 (t test: $P < 0{\cdot}001$).

The theory we have used is certainly adequate for the data, but is not unique, and indeed, any theory for which the fluctuation–dissipation theorem holds would be equally good at the formal level. If the state of end-plate channels is completely specified by only a single variable conductance for example, all that is required for the fluctuation–dissipation theorem to hold is that the system be macroscopically memoryless (Stevens, 1972). Thus, our results, taken by themselves, are consistent with a rather general class of possible theories. Although we have not been able to formulate a plausible alternative to the theoretical scheme used, we must emphasize that the rather striking agreement between theory and experiment presented here cannot be taken as final proof of our theory; it merely shows that the theory is consistent.

As indicated earlier, the interpretation one places on the conductance spectra we have studied depends upon the precise assumptions made about the system. For example, we have assumed that the binding of ACh to the receptor is rapid and voltage independent, whereas the subsequent con-

formational change is slower and field-dependent; in terms of this model, the physical significance of the cut-off frequency f_c of our conductance fluctuation spectra is intimately related to the dipole moment of the hypothetical gating molecule. Guided by the rapid kinetic studies of enzyme-substrate interactions (Eigen & Hammes, 1963; Hammes, 1968*b*), we have chosen to make the binding step rapid and the conformational change rate limiting, but the same formal theory would result from the opposite assumption, that is, a slow and voltage dependent binding of ACh to its receptor and very rapid conformational change. This second interpretation would be entirely consistent, but the rate constant α would no longer be related to the gating molecule's dipole moment.

We have assumed that the end-plate channels have only two states, open and closed. Although a large number of models can be constructed consistent with the e.p.c. spectra, they would not in general yield a fluctuation–dissipation theorem. The two-state model we have used is not, however, unique in giving such a theorem. For example, if it were assumed that a channel opened instantaneously and then decreased its conductance exponentially, all of our data would be equally well explained, at least at the formal level. With this model, however, the quantity γ, that is, the conductance of a single open channel, might well be different. For example, if γ is taken as the channel conductance immediately after opening, the exponential model would yield a value of γ twice that of the theory we have used here.

Support for the use of a two-state model to represent the single-channel gating mechanism is available from rapid kinetics studies of enzyme systems as well as from studies of artificial membranes. Protein conformation changes have been adequately described by schemes in which the molecule rapidly switches between stable states (Eigen & Hammes, 1963; Hammes 1968*a*, *b*; Chock, 1971; Gutfreund, 1971). This, coupled with the suggestive evidence from artificial membrane work in which the individual channel conductance time courses can be observed and always appear as square pulses, lead us to support the discrete conductance hypothesis (Hladky & Haydon, 1970; Bean, 1972; Ehrenstein *et al.* 1970; Gordon & Haydon, 1972; LaTorre, Ehrenstein & Lecar, 1972). Rang (1971) has also suggested that a discrete model would better satisfy work on dose–response characteristics of the receptor.

Katz and Miledi have previously estimated the conductance of a single channel to be approximately 10^{-10} mhos, a value 3–5 times larger than we obtained. Although the precise assumptions (e.g. two-state channel *vs.* exponential decay of conductance) used by Katz and Miledi in making their calculation of γ are not clear to us, differences in experimental technique and methods of data analysis alone are probably adequate to

account for a discrepancy of this magnitude. Our estimate of γ, however, is considerably different from the value reported by Kasai & Changeux (1971); Katz & Miledi (1972) have already discussed reasons for this rather large discrepancy. We feel that our estimate of γ is the most reliable currently available, but must emphasize that this quantity is accurate only insofar as the theory used to calculate it is satisfactory, so that a more precise evaluation of this parameter must await the acceptance of a physical model for end-plate response.

The low concentration limit

In our development of the equations used to interpret the observed fluctuation spectra, we have supposed (see p. 669), as was assumed earlier (Magleby & Stevens, 1972*b*), that the post-junctional membrane was subjected only to low concentrations of ACh in the sense that only a very small fraction of the receptors were, at any moment, combined with ACh. In this low concentration limit, the number of receptors not bound to ACh is effectively constant, and the random process which describes ACh-receptor interaction may be assumed to be Poisson. Unfortunately, no information independent of the results obtained here is available to permit evaluation of this assumption. We can, however, check the consistency of the assumption with our data. For the low concentration limit, because the underlying process is then Poisson, the variance of conductance fluctuations should be proportional to the mean conductance, whereas if appreciable number of receptors were combined with ACh at higher ACh concentrations, the slope of the variance *vs.* mean conductance should decrease for the higher mean conductances. Over the range of mean end-plate conductances investigated in our experiments, variance was indeed proportional to mean conductance as required by our assumption of low ACh concentrations (see Fig. 3).

It should be stressed that 'low concentrations' does not in this context imply unphysiological ACh doses: our iontophoretically applied ACh produced end-plate conductance increases up to 4 or 5 μmhos, values that are comparable to the peak conductance of normally evoked end-plate currents under the conditions of our experiments.

If it is assumed that 10^8–10^9 channels are present at a frog end-plate (Miledi & Potter, 1971), our estimated single-channel conductance of 3×10^{-11} mho and peak end-plate conductance of 4×10^{-6} mho would imply that only 0·01–0·1 % of the total channels normally are open at the time of peak end-plate conductances. This calculation indicates that our results are internally consistent in that the value of γ obtained with the assumption of low ACh concentrations yields, in turn, appropriate estimates for the fraction of channels which open during an e.p.c.

Sources of errors

Errors in our analysis could arise through serious contamination of ACh induced fluctuations with noise from other sources, in which case our spectra would reflect properties of the system other than those we wish to investigate, or from a failure of the voltage clamp system to measure accurately fluctuations in end-plate conductance. The following arguments suggest that our spectra are not of artificial origin and further that they are not appreciably distorted by the measurement system we have used.

A variety of observations indicate that the e.p.c. fluctuation spectra reported here do in fact reflect properties of the ACh receptor controlled ionic channels. The fluctuations are only observed during ACh application and are highly localized to the end-plate region as defined by the presence of large, fast rising e.p.c.s and m.e.p.c.s. Movement of the voltage clamping micro-electrodes even a few hundred microns away from this region causes a large decrease in σ_I^2 and the ACh noise is unobservable in non end-plate regions of the muscle fibre. The ACh induced noise variance is proportional to the mean end-plate current and increases directly with increased iontophoresis current (Fig. 3). A well-defined equilibrium potential can be measured for the ACh spectrum (where σ_I^2 is at a minimum), and this is the same as that found for e.p.c.s and spontaneous m.e.p.c.s, suggesting identical ionic mechanisms.

One possible source of contaminating noise is the spontaneous occurrence of m.e.p.c.s; we feel, however, that this source did not make a significant contribution to our spectra. Contamination of the spectral estimates by spontaneous m.e.p.c.s was minimized by selecting end-plates with undamaged presynaptic terminals (as judged by m.e.p.c. rate) and by working at relatively low temperature. Often m.e.p.c.s could be detected above the ACh noise and records were screened before spectral analysis to avoid their presence. We have calculated the effect of m.e.p.c.s on the spectral estimates by calculation of the added spectrum $\tilde{S}(f)$ from the Fourier transform of the covariance, $C(t)$, of m.e.p.c.s. If $m(t)$ represents a single m.e.p.c. and ν the rate of random occurrence then

$$C(t) = \nu \int_0^\infty m(\tau) m(t+\tau)\, \mathrm{d}t,$$

$$\tilde{S}(f) = R_e \mathscr{F}\{C(t)\} = 2\nu \left| \int_0^\infty m(\tau) \mathrm{e}^{-i2\pi\tau f}\, \mathrm{d}\tau \right|^2.$$

If $m(t)$ rises instantaneously to a value M and decays exponentially with rate α: $m(t) = M\mathrm{e}^{-\alpha t}$, $t \geqslant 0$ then,

$$\tilde{S}(f) = 2\nu \frac{M^2}{\alpha^2 + (2\pi f)^2}.$$

We estimate that after screening the records $\nu_{max} = 0{\cdot}2$/sec at 8° C. For $M = 1 \times 10^{-9}$ A (see Fig. 2 and Gage & McBurney (1972)) and $\alpha = 0{\cdot}14$ (msec^{-1}) at $V = -50$ mV (see Fig. 9), $\tilde{S}(O) = 2{\cdot}0 \times 10^{-23}$ A^2 sec for the m.e.p.c. contribution. Thus, since $\tilde{S}(O) \approx 10^{-21}$ A^2 sec for the ACh noise (see Fig. 4), the maximum contamination of the e.p.c. spectrum by undetected m.e.p.c.s is less than 1·0 %. Further evidence that ACh fluctuations are not a result of spontaneous m.e.p.c.s is given by the presence of ACh noise in denervated end-plates (Katz & Miledi, 1972).

Nor does it seem likely that ACh fluctuations are due to the iontophoresis technique since bath application gave equivalent results (Katz & Miledi, 1972). Further, we monitored the iontophoresis current and replaced electrodes showing appreciable drift or noise above that expected from thermal properties of the micro-electrode impedance. Positioning the electrode relatively far (approximately 50 μm) from the end-plate effectively inserted a low pass diffusion filter on the end-plate ACh concentration. Results were identical for close and far iontophoresis electrodes.

The adequacy of the voltage clamp system used in these experiments has been considered elsewhere (Magleby & Stevens, 1972*a*); several observations reported here provide additional evidence that our apparatus has in fact accurately reflected the end-plate conductance changes.

The estimates of single channel conductance γ did not vary significantly with mean end-plate current μ_I (see p. 679). If voltage control were not well maintained, however, γ would decrease as the mean current increased because errors in voltage control vary in proportion to the magnitude of the conductance change; in fact, we have observed such non-constancy of γ on occasions when the feed-back amplifier gain was not set to sufficiently large values. The fact that γ generally did not depend on mean current indicates, then, that voltage control was adequate over the range of conductance increases encountered in our preparations.

Since end-plate regions can occupy a significant fraction of a space constant, and particularly since the effective space constant is shorter for more rapidly varying signals, it is possible for errors to arise from the failure to control adequately voltage over the entire region of end-plate conductance increase (see p. 659). Gage & McBurney (1972) have noted a difference between the decay constant for the m.e.p.c.s they studied and the decay constants published in the literature for e.p.c.s, and they conjecture that this difference might be due to just such failure to achieve uniform control over the whole end-plate region. We have not observed such a discrepancy in the instances where the e.p.c.s and m.e.p.c.s were studied at the same end-plate. Thus, the fact that presumably localized and widespread conductance increases at the end-plate behaved in the same manner is further evidence for the adequacy of our voltage clamp.

Effects of pre-treatment with hypertonic solutions

Hypertonic pretreatment of the muscle to disrupt excitation-contraction coupling affected some membrane properties while leaving others intact. Resting potentials were below normal (-40 to -70 mV) and the equilibrium potential, as determined from e.p.c. reversals, shifted to near 0 mV. We have ascribed this effect to a loss of internal K^+ during hypertonic tubule disruption. Evidence for this hypothesis is based upon the suggestion that membrane $1/f$ noise is due to K^+ ion flow (Verveen & Derksen, 1968; Poussart, 1971). We have observed that the magnitude of $1/f$ noise has a minimum which occurs at higher membrane potentials in glycerol fibres than in normal ones indicating a positive displacement of the K^+ equilibrium potential. The input resistance of the muscle fibres, however, recovered to approximately normal values after osmotic shock.

ACh receptor function appeared to be unaffected by glycerol or ethylene glycol pre-treatment. This conclusion is supported by the fact that ACh fluctuation spectra taken in untreated fibres, over a limited range of V, exhibited the same characteristics as pretreated muscles. In addition, e.p.c. decay kinetics were the same in glycerol fibres and in untreated muscle where contraction was blocked by curare (Magleby & Stevens, 1972*b*). Thus, we have seen no evidence that subjecting muscles to the hypertonic solutions alters the properties we wish to investigate, although we cannot of course be confident that gating mechanisms are entirely unaffected by this procedure.

Summary of the proposed physical gating mechanism

In this work we have characterized the end-plate conductance fluctuations which result from constant applications of ACh: the form of the spectra is accurately summarized by eqn. (4), a description containing two parameters. The first of these parameters, the cut-off frequency f_c, varies exponentially with voltage, whereas the second parameter γ, which reflects an appropriately normalized amplitude of the spectrum (see eqn. (6)), shows no significant dependence on voltage. The declining phase of both e.p.c.s and m.e.p.c.s is exponential, and the rate constant α which specifies the form of this exponential also depends exponentially on voltage. Our results show that the cut-off frequency of e.p.c. spectra and the decay constant for m.e.p.c.s are related by $f_c = \alpha_e/2\pi$.

The physical model we have adopted will account quantitatively for these observations. According to our picture, a gating macromolecule guards an ion selective channel with an open conductance of about 3×10^{-11} mho which permits the passage of Na and K ions. This gating molecule can be in either of two principal conformations, one of which

permits ion flow through the channel and the other of which prevents it. When ACh binds to its receptor, the energy barrier between the open and closed conformations is reduced so that the channel opens and closes according to a random process. At 8° C and 0 mV the channel, once open, remains open for 6·5 msec on the average; at -100 mV the energy barrier for a conformational transition from open to closed is increased by about 0·3 kcal/mole, because of the coupling of the membrane electric field to the gating molecule's dipole moment, and the channel remains open for an average of 11 msec. During this open time an average of 2×10^5 ions pass through the channel at a rate of about 2×10^7 ions/sec. A single quantum of transmitter opens approximately 1700 channels and, under the conditions of our experiments, with a quantal content of approximately 80, about 135,000 are open at the peak of a normal e.p.c.

Experiments reported here then support a very specific model of gating behaviour in that we are able to account quantitatively for a rather wide range of observations of end-plate behaviour. A final evaluation of the physical reality of this picture must, however, await further and more direct experimental investigations.

APPENDIX

This appendix contains brief derivations of relations used in the text; some of this material has been presented partially, or in a different form, by Magleby & Stevens (1972*b*) and Stevens (1972).

Probabilistic behaviour of an end-plate channel

Suppose that an end-plate channel may have only two conductance states with an open conductance γ and a zero closed conductance, that the transition of transmitter-receptor complexes occur according to a Poisson process with an opening rate β and a closing rate α, and that channels operate independently. We restrict attention to the low ACh concentration case in which the probability of an open channel is small and the fraction of channels with n AChs bound to their receptors (n is the number of AChs required for a channel to open) may be assumed to be $Kc^n(t)$; K is the ACh-receptor binding constant and $c(t)$ is the cleft ACh concentration at time t. Let $p(k, t)$ be the probability that a channel is open at time t, given an initial state k (k may be either o = open or c = closed) at time $t = 0$. The conditional probability $p(k, t)$ then is governed by the equation

$$\frac{\mathrm{d}p(k, t)}{\mathrm{d}t} = -(\alpha + \beta K c^n(t))\, p(k,t) + \beta K c^n(t).$$

Since we have assumed that only a small fraction of the channels are open

at any time, $\beta K c^n(t)$ must always be small compared to α so that this equation becomes

$$\frac{dp(k,t)}{dt} = -\alpha p(k,t) + \beta K c^n(t). \tag{A 1}$$

We now derive equations first for the mean end-plate conductance and then for the e.p.c. spectrum.

Average end-plate conductance

The mean end-plate conductance $g(t)$ is given by the fraction of channels that are open times the maximum possible conductance:

$$g(t) = P(t)\gamma N.$$

Here $P(t)$ is the probability that a channel is open (irrespective of its state at time zero) and N is the total number of end-plate channels. If, for convenience, the initial conductance $g(O)$ is assumed to be zero so that initially all channels are closed, then,

$$P(t) = p(c,t).$$

Multiplication of both sides of eqn. (A 1) with $k = c$ by γN thus yields an expression for mean end-plate conductance,

$$\frac{dg(t)}{dt} = -\alpha g(t) + \beta N \gamma K c^m(t) \tag{A 2}$$

which has the solution:

$$g(t) = \beta N \gamma K \int_0^t c^n(\tau)\, e^{-\alpha(t-\tau)} d\tau. \tag{A 3}$$

According to this last result, e.p.c.s decay exponentially with a decay constant α after $c(t)$ has declined essentially to zero; Magleby & Stevens (1972*a*) have maintained $c(t)$ is negligible for the entire declining phase of e.p.c.s and that e.p.c. decays therefore provide an estimate of α.

Spectrum of e.p.c. fluctuations

The spectral density $S(f)$ of e.p.c. fluctuations is most conveniently calculated by Fourier transforming N times the covariance function $C_1(t)$ for the behaviour of a single channel. Covariance is defined to be

$$\begin{aligned} C_1(t) &= E\{I_1(O)I_1(t)\} - E\{I_1(\infty)\}^2 \\ &= E\{(V-V_{eq})^2\, g_1(O)g_1(t)\} - E\{(V-V_{eq})g_1(\infty)\}^2, \end{aligned}$$

when $E\{\ \}$ indicates expectation, $g(t)$ is the conductance of the channel at t, $I_1(t)$ is the single channel current at t, V is the membrane potential and V_{eq} the equilibrium potential. $C_1(t)$ thus becomes, for steady-state fluctuations with constant ACh concentration c,

$$C_1(t) = \gamma^2(V-V_{eq})^2 p(o,\infty)\, p(o,t) - \gamma^2(V-V_{eq})p^2(o,\infty).$$

By solving eqn. (A 1) for $p(c, t)$, the covariance function is found to be

$$C_1(t) = \gamma^2(V-V_{eq})^2\beta K c^n e^{-\alpha t}, (t \geqslant 0).$$

The spectral density, obtained from the real part of the Fourier transform of $NC_1(t)$, is thus

$$S(f) = \frac{2N\gamma^2(V-V_{eq})^2\beta K c^n/\alpha}{1+(2\pi f/\alpha)^2}.$$

Since the mean e.p.c. μ_I is $N(V-V_{eq})\,Kc^n$, eqn. (4) of the text results:

$$S(f) = \frac{2\mu_I\gamma(V-V_{eq})/\alpha}{1+(2\pi f/\alpha)^2}. \qquad (A\,4)$$

Integration of (A 4) over all frequencies yields the variance of e.p.c. fluctuations and relates this variance to the mean e.p.c. If the variance and mean of current fluctuations are converted into a variance and mean of conductance fluctuations (through Ohm's law), (A 4) implies that the conductance variance is proportional to the mean conductance with the proportionality constant γ(eqn. (2)); thus γ may be estimated either from $S(f)$ directly or from its integrated form.

REFERENCES

ADRIAN, R. H., CHANDLER, W. K. & HODGKIN, A. L. (1970). Voltage clamp experiments in striated muscle fibres. *J. Physiol.* **208**, 607–644.

ANDERSON, C. R. & STEVENS, C. F. (1972). Membrane conductance fluctuations associated with acetylcholine depolarization of frog neuromuscular junction. *Biophys. Soc. Annu. Meet. Abstr.* **12**, 77a.

ANDERSON, C. R. & STEVENS, C. F. (1973). Conductance and voltage dependence of acetylcholine sensitive ionic channels in voltage clamped endplate. *Biophys. Soc. Annu. Meet. Abstr.* **13**, 71a.

ASELTINE, J. A. (1958). *Transform Method in Linear System Analysis.* New York: McGraw-Hill.

BEAN, R. C. (1972). Multiple conductance states in single channels of variable resistance lipid bilayer membranes. *J. membrane Biol.* **7**, 15–28.

BENDAT, J. S. & PIERSOL, A. G. (1971). *Random Data: Analysis and Measurement Procedures.* New York: Wiley Interscience.

CHOCK, P. B. (1971). Relaxation methods and enzymology. *Biochimie* **53**, 161–172.

CONNOR, J. A. & STEVENS, C. F. (1971). Inward and delayed outward membrane currents in isolated neural somata under voltage clamp. *J. Physiol.* **213**, 1–19.

COOLEY, J. W. & TUKEY, J. W. (1965). An algorithm for the machine calculation of Fourier series. *Math. of Computn* **19**, 297–301.

DULHUNTY, A. F. & GAGE, P. W. (1973). Electrical properties of toad sartorius muscle fibres in summer and winter. *J. Physiol.* **230**, 619–641.

EHRENSTEIN, G., LECAR, H. & NOSSAL, R. (1970). The nature of the negative resistance in bimolecular lipid membranes containing excitability-inducing material. *J. gen. Physiol.* **55**, 119–133.

EIGEN, M. & HAMMES, G. G. (1963). Elementary steps in enzyme reactions studied by relaxation spectrometry. *Adv. Enzymol.* **25**, 1–38.

EISENBERG, R. S., HOWELL, J. N. & VAUGHAN, P. C. (1971). The maintenance of resting potentials in glycerol-treated muscle fibres. *J. Physiol.* **215**, 95–102.

FALK, G. & FATT, P. (1964). Linear electrical properties of striated muscle fibres observed with intracellular electrodes. *Proc. R. Soc.* B **160**, 69–123.

FATT, P. & KATZ, B. (1951). An analysis of the end-plate potential recorded with an intracellular electrode. *J. Physiol.* **115**, 320–370.

FATT, P. & KATZ, B. (1952). Spontaneous subthreshold activity at motor nerve endings. *J. Physiol.* **117**, 109–128.

FISHMAN, H. (1972). Excess noise from small patches of squid axon membrane. *Biophys. Soc. Annu. Meet. Abstr.* **12**, 119a.

FISHMAN, H. (1973). Relaxation spectra of potassium channel noise from squid axon membranes. *Proc. natn. Acad. Sci.* **70**, 876–879.

FRANKENHAEUSER, B. & MOORE, L. E. (1963). The effect of temperature on the sodium and potassium permeability changes in myelinated nerve fibres of *Xenopus laevis*. *J. Physiol.* **169**, 431–437.

GAGE, P. W. & ARMSTRONG, C. M. (1968). Miniature end-plate currents in voltage clamped muscle fibres. *Nature, Lond.* **218**, 363–365.

GAGE, P. W. & EISENBERG, R. S. (1969). Capacitance of the surface and transverse tubular membrane of frog sartorius muscle fibers. *J. gen. Physiol.* **53**, 265–278.

GAGE, P. W. & MCBURNEY, R. N. (1972). Miniature end-plate currents and potentials generated by quanta of acetylcholine in glycerol-treated toad sartorius fibres. *J. Physiol.* **226**, 70–94.

GORDON, L. G. M. & HAYDON, D. A. (1972). The unit conductance channel of alamethicin. *Biochim. biophys. Acta* **255**, 1014–1018.

GUTFREUND, H. (1971). Transients and relaxation kinetics of enzyme reactions. *A. Rev. Biochem.* **40**, 315–344.

HAMMES, G. G. (1968*a*). Relaxation spectrometry of biological systems. *Adv. Protein Chem.* **23**, 1–58.

HAMMES, G. G. (1968*b*). Relaxation spectrometry of enzymatic reactions. *Acc. Chem. Res.* **1**, 321–329.

HLADKY, S. B. & HAYDON, D. A. (1970). Discreteness of conductance change in bimolecular lipid membranes in the presence of certain antibiotics. *Nature, Lond.* **225**, 451–453.

HOWELL, J. N. & JENDEN, D. J. (1967). T-tubules of skeletal muscle: morphological alterations which interrupt excitation contraction coupling. *Fedn Proc.* **26**, 553.

KASAI, M. & CHANGEUX, J. P. (1971). In vitro excitation of purified membrane fragments by cholinergic agonists. III. *J. membrane Biol.* **6**, 58–80.

KATZ, B. & MILEDI, R. (1970). Membrane noise produced by acetylcholine. *Nature, Lond.* **226**, 962–963.

KATZ, B. & MILEDI, R. (1971). Further observations on acetylcholine noise. *Nature, New Biol.* **232**, 124–126.

KATZ, B. & MILEDI, R. (1972). The statistical nature of the acetylcholine potential and its molecular components. *J. Physiol.* **224**, 665–700.

KATZ, B. & MILEDI, R. (1973). The characteristics of 'end-plate noise' produced by different depolarizing drugs. *J. Physiol.* **230**, 707–717.

KATZ, B. & THESLEFF, S. (1957). A study of the 'desensitization' produced by acetylcholine at the motor end-plate. *J. Physiol.* **138**, 63–80.

KORDAS, M. (1969). The effect of membrane polarization on the time course of the end-plate current in frog sartorius muscle. *J. Physiol.* **204**, 493–502.

KORDAS, M. (1972*a*). An attempt at an analysis of the factors determining the time course of the end-plate current. I. The effects of prostigmine and of the ratio of Mg^{2+} to Ca^{2+}. *J. Physiol.* **224**, 317–332.

KORDAS, M. (1972*b*). An attempt at an analysis of the factors determining the time course of the end-plate current. II. Temperature. *J. Physiol.* **224**, 333–348.

KUBO, R. (1957). Statistical mechanical theory of irreversible processes. I. General theory and simple application to magnetic and conduction problems. *J. phys. Soc. Japan* **12**, 570–586.

KUNO, M., TURKANIS, S. A. & WEAKLEY, J. N. (1971). Correlation between nerve terminal size and transmitter release at the neuromuscular junction of the frog. *J. Physiol.* **213**, 545–556.

LATORRE, R., EHRENSTEIN, G. & LECAR, H. (1972). Ion transport through excitability-inducing material (EIM) channels in lipid bilayer membranes. *J. gen. Physiol.* **60**, 72–85.

MCMAHAN, U. J., SPITZER, N. C. & PEPER, K. (1972). Visual identification of nerve terminals in living isolated skeletal muscle. *Proc. R. Soc.* B **181**, 421–430.

MAGAZANIK, L. G. & VYSKOČIL, F. (1970). Dependence of acetylcholine desensitization on the membrane potential of frog muscle fibre and on the ionic changes in the medium. *J. Physiol.* **210**, 507–518.

MAGLEBY, K. L. & STEVENS, C. F. (1972*a*). The effect of voltage on the time course of end-plate currents. *J. Physiol.* **223**, 151–171.

MAGLEBY, K. L. & STEVENS, C. F. (1972*b*). A quantitative description of end-plate currents. *J. Physiol.* **223**, 173–197.

MILEDI, R. & POTTER, L. T. (1971). Acetylcholine receptors in muscle fibres. *Nature, Lond.* **233**, 599–603.

PEPER, K. & MCMAHAN, U. J. (1972). Distribution of acetylcholine receptors in the vicinity of nerve terminals on skeletal muscle of the frog. *Proc. R. Soc.* B **181**, 431–440.

POUSSART, D. J. M. (1971). Membrane current noise in lobster axon under voltage clamp. *Biophys. J.* **11**, 211–234.

RANG, H. P. (1971). Drug receptors and their function. *Nature, Lond.* **231**, 91–96.

SEVCIK, C. & NARAHASHI, T. (1972). Electrical properties and excitation contraction coupling in skeletal muscle treated with ethylene glycol. *J. gen. Physiol.* **60**, 221–236.

SIEBENGA, E. & VERVEEN, A. A. (1972). Membrane noise and ion transport in the node of Ranvier. *Biomembranes* **3**, 473–482.

STEVENS, C. F. (1972). Inferences about membrane properties from electrical noise measurements. *Biophys. J.* **12**, 1028–1047.

TAKEUCHI, A. & TAKEUCHI, N. (1959). Active phase of frog's end-plate potential. *J. Neurophysiol.* **22**, 395–411.

VERVEEN, A. A. & DERKSEN, H. E. (1968). Fluctuation phenomena in nerve membrane. *Proc. I.E.E.E.* **56**, 906–916.

Voltage clamp analysis of acetylcholine produced end-plate current fluctuations at frog neuromuscular junction

C. R. Anderson and C. F. Stevens

J. Physiol. 1973;235;655-691